Determination of Organic Contaminants Concentration on the Silica Surface by Lateral Force Microscopy

N. Ivliev [1,2], V. Kolpakov [2], S. Krichevskiy [2], N. Kazanskiy [1,2]

[1] Image Processing Systems Institute of RAS, Branch of the FSRC "Crystallography and Photonics" RAS
E-mail: ivlievn@gmail.com
[2] Samara National Research University
Samara, Russia

Received: 25.11.2016

Abstract. We present a method for determining the concentration of organic contaminants on the silica surface by using lateral force maps and surface topology images obtained with scanning probe microscopy. In this study, we optimized the scanning frequency to increase image contrast and facilitate interpreting data obtained. We also proved experimentally that the sensitivity of the method reaches 10^{-11} g/cm^2.

Keywords: concentration of organic contaminants, surface, lateral force

INTRODUCTION

Monitoring the surface cleanliness of semiconductor and dielectric substrates finds wide application in micro- and nanoelectronics [1–3], diffractive optics [4, 5], and nanophotonics [6]. This is necessitated by adsorbed contamination, which causes changes in electro-physical surface properties [7, 8], deteriorates the adhesion of applied process layers [9, 10], increases the thickness of surface oxide during thermal oxidation [11], and thus deteriorates the operating characteristics of the fabricated element or results in its failure.

Micro- and nanominiaturization of fabricated structures leads to higher requirements for the cleanliness of substrate surfaces. Today the allowable carbon-atom concentration for fabricating semiconductor devices is 10^{12} atoms/cm^2 [12]. The value is that low because carbon atoms have a significant effect on local surface conductivity. According to [11, 13, 14], those organic-compound molecules that, even under clean-room conditions, come from plasticizers in plastic products (such as polyethylene packaging for substrates and Petri dishes) present carbon contamination that is hardest to remove. Therefore, monitoring such contamination is a priority.

Using modern techniques based on mass spectrometry [15, 16] and multiple internal reflection infrared spectroscopy [1, 17] to assess the concentration of organic contaminants makes it possible to attain the required sensitivity. But those techniques do not yield information on how the molecules are distributed across the surface, although that information is needed in the case of nonuniform contamination.

Studies [18–20] present AFM (atomic force microscopy) methods based on the registration of lateral forces (LF) acting on the atomic force microscope's probe that is in constant con-tact with the surface. Probe scanning along a line in two directions rules out the forces caused by surface roughness. Thus, LF maps obtained from the measurement result from the action of adhesion bonds between the probe and the surface, and the bonds energies characterize the chemistry of the phase boundary. This can be used for assessing the concentration and distribution of surface contaminants.

Thus, this paper aims to study the local tribological properties of substrates with the AFM method of lateral forces in order to realize the method for determining the concentration of organic contaminants.

THEORETICAL ANALYSIS

Molecules of organic contaminants adsorb on the surface and interact with electronic states at the surface. The energy of that interaction corresponds to the van der Waals forces and depends on the structure of adsorbed molecules [21].

Dioctyl- and dibutyl phthalate are the most commonly used industrial plasticizers. The presence of C=O and −OH groups in the molecular structure of these cyclic hydrocarbons determines their strong polarity, and the polarity causes the surface and the contaminant to bond. The energy of that bond is, in this case, determined by the hydrogen bridges formed with the −OH groups of the native oxide as well as by the orientation interaction between the dipole and the surface. The value of the orientation interaction can be calculated with the expression [22]:

$$E_{or} = -\frac{2p_1p_2}{r^3}, \tag{1}$$

where p_1, p_2 – dipole moments of a contaminant molecule and the −OH group, respectively; r – length of the O···HO hydrogen bond.

The energy of the O···HO hydrogen bond is 21.5 kJ/mol [23]. Therefore, given the orientation interaction calculated with (1), the aggregate bond energy of the substances in question reaches 50 kJ/mol, a value close to a stable chemical bond that is difficult to break. Therefore, the force that acts on the surface from the AFM probe during the measurement and that equals dozens of nanonewtons cannot cause dioctyl- and dibutyl phthalate molecules to desorb.

AFM methods make it possible to register only the molecular concentration of contaminants – that is, the methods cannot measure the concentration of carbon atoms in atoms per square centimeter. That dimension is comparable with the dimension of the mass concentration of organic contaminants under ISO 14644-10–2013 in grams per square centimeter through the use of the expression [24, 25]:

$$C_{mol} = \frac{C_{at}M}{N_AN_c}, \tag{2}$$

where C_{mol} – mass concentration of organic contaminants; C_{at} – concentration of carbon atoms; N_A – Avogadro constant; Nc – number of carbon atoms in a contaminant molecule.

The mass concentrations of dioctyl- and dibutyl phthalate calculated with (2) that correspond to 10^{12} atoms/cm^2 are equal to $2.7\cdot10^{-11}$ and $3\cdot10^{-11}$ g/cm^2, respectively. For this reason, the value 10^{-11} g/cm^2 is the required sensitivity level for the present method.

EXPERIMENTAL TECHNIQUE

Experimental research into local tribological surface properties as a function of the concentration of organic contaminants necessitates forming surfaces with varying degrees of contamination, a procedure that consists of three stages.

The first stage consists in cleaning substrate surfaces to the degree of production-grade cleanliness. This is accomplished through rough and final cleaning. Rough cleaning, which serves to remove primary contaminants from the surface, was accomplished with the chemical technique of boiling substrates alternately in alkaline and alcohol solutions such as NaOH and C_3H_8O for ten-minute periods. Final cleaning was accomplished by using Solurus 950, a plasma cleaning system from Gatan, in Ar/O_2 plasma with a gas ratio of 75/25%, respectively, as recommended by the manufacturer. The substrates were irradiated for 4 min at 50 W, the maximal generator power.

The second stage consists in contaminating, by using a special device, the cleaned surfaces with dibutyl-phthalate molecules to the concentration corresponding to the monomolecular level, under the method described in [5].

In the third stage, final plasma cleaning is repeated to adjust the degree of surface cleanliness by changing the irradiation time, ranging from 0 to 4 min in increments of 0.5 min.

The lateral forces of the prepared specimens were then studied in contact mode with Solver PRO-M, a scanning probe microscope from NT-MDT.

Measurements in contact mode are characterized by the high possibility of the probe surface becoming contaminated (Fig. 1a; the contamination is shown with arrows). Because of this, before each measurement took place, the probe was cleaned with Ar/O_2 plasma under the same conditions as those for the substrates. Figure 1b shows the cleaning results. Large contaminant fractions are not observed in the figure, which indicates that the initial surface properties were restored.

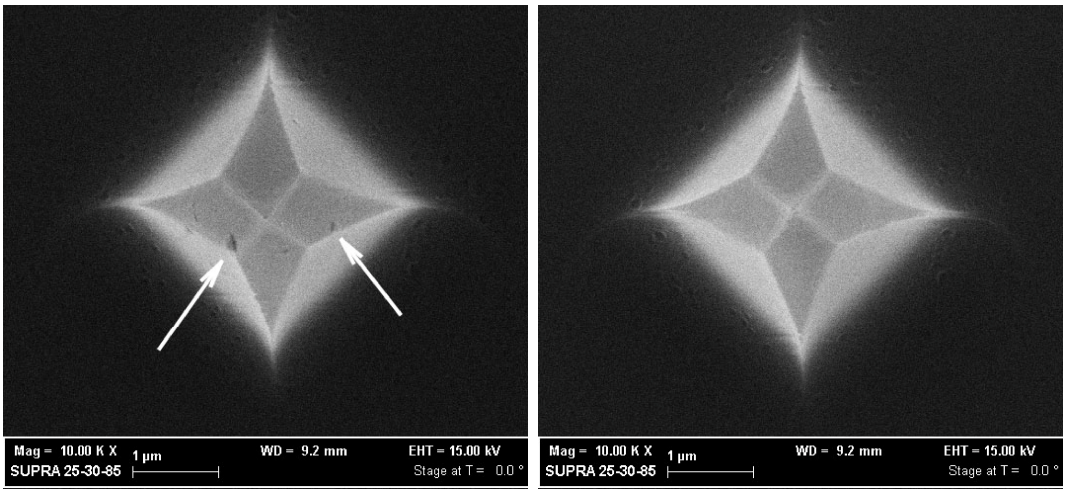

(a) (b)

Figure 1. SEM images of the CSC12 AFM probe: (a) before and (b) after cleaning

The specimens were 1 cm^2 SiO_2 NanoInk wafers used in dip-pen nanolithography. A feature of those wafers is low surface roughness, making it possible to minimize the torsional deflection of the cantilever caused by the local inclination of the surface and thus minimize the error of LF measurement.

RESULTS AND DISCUSSION

Figure 2a shows an AFM image of an LF map obtained by scanning, at a frequency of 0.5 Hz, a 1×1 μm area on the surface of a substrate that has gone through the full cleaning process. The area in the image exhibits a uniform structure and does not have sharply contrasting fragments. But when the scanning frequency was increased to 1 Hz, the LF map developed well-pronounced grains (Fig. 2c) corresponding to roughness protrusions (Fig. 2d). At the same time, the roughness values did not change in relation to the map obtained at 0.5 Hz (Fig. 2b). This rules out differences in the surface structure in different substrate areas.

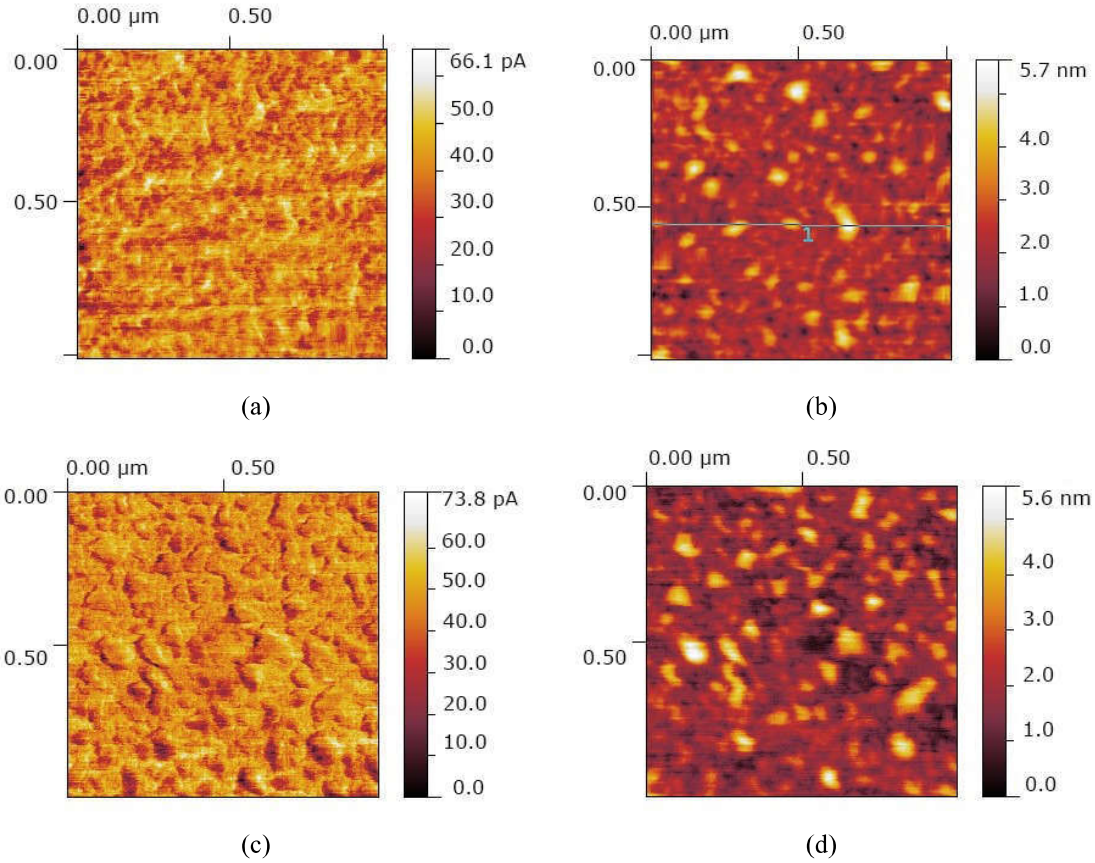

Figure 2. AFM images showing the surface of a cleaned substrate, obtained at 0.5 Hz (*a* shows an LF map and *b*, the surface relief) and 1 Hz (*c* shows an LF map and *d*, the surface relief)

The maximal LF value at 1 Hz (Fig. 2*c*) corresponds to the maximal photodetector current, 73.8 pA, on the gradient scale. Figure 2*c* shows that the value increased by 7.7 pA – about 11% of the initial value – in relation to that in Figure 2*a*. The change cannot be coincidental because scanning takes place in constant-force mode.

Thus, the only possible cause of both the grains and the increase in the torsional deflection of the cantilever when the scanning rate is increased is the action of the capillary forces due to the viscosity of the adsorbed water film; and the homogeneity of the structure confirms indirectly that the surface is clean to a degree conforming to production-grade cleanliness.

Figures 3*a* and 3*b* show AFM images of a substrate surface cleaned with Ar/O_2 plasma for a period of $t = 2.5$ min.

Dark spots on the LF map (Fig. 3*a*) correspond to the minimal torsional deflection of the cantilever for this area of the surface. In this case, the maximal photodetector current corres-

ponding to the maximal cantilever deflection equals 134 pA, a value 2 times higher than the current for the clean surface (Fig. 2*a*). This indicates a 2-fold decrease in the minimal cantilever deflection. The location of dark spots on the LF map corresponds to the regions of the largest heights in the image showing the surface relief (Fig. 3*b*). This presents the conclusion that the dark spots correspond to molecular contaminants that act as a lubricant between the probe and the substrate surface.

When the scanning frequency is increased to 1 Hz (Fig. 3*c*), the range of the registered torsional deflection significantly broadens because of the absence of adsorbed water molecules on the surfaces of molecular-contaminant islets. This causes the color contrast of the image to increase and thus simplifies analyzing the organic-contaminant concentration, which is characterized by the volume of protrusions in the relief images (Fig. 3, *b* and *d*), corresponding to the dark areas on the LF maps. Contaminated regions can be allocated by the threshold principle: the higher the image contrast, the sharper the threshold.

Because a further increase in the scanning frequency does not improve the image contrast significantly but instead increases the wear of the probe, it is inadvisable.

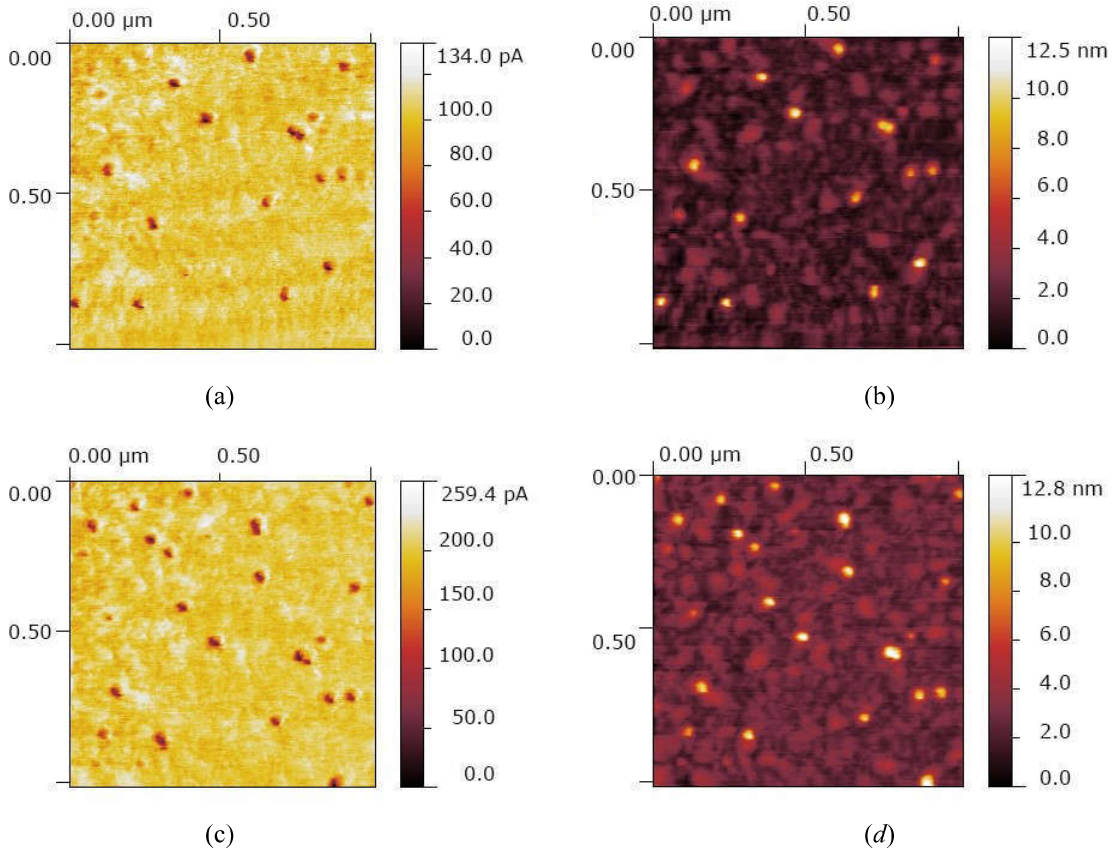

Figure 3. AFM images of contaminated surfaces, obtained at 0.5 Hz (*a* shows an LF map and *b*, the surface relief) and 1 Hz (*c* shows an LF map and *d*, the surface relief)

To determine contaminant concentrations with LF maps, we developed an application program to allocate light spots in relief images so that the spots geometrically correspond to the dark spots on LF maps and to determine the volume of the areas so allocated. To calculate contaminant concentrations, we used the equation:

$$C_a = \frac{\rho V_a}{S}, \qquad (3)$$

where ρ – adsorbate density, and it is equal to 0.982 g/cm^3 for dibutyl phthalate; S – surface area of the measured surface; V_a – volume of the allocated areas.

Figure 4 shows the relationship between the concentration of organic contaminants and the irradiation time. The relationship was obtained with the present method. For each contamination level, concentrations were measured in three surface points, and their averages were recorded on a plot. From the relationship in Figure 4, it follows that the concentration ranges between 10^{-11} and 10^{-8} g/cm^2. Note that the lower limit of this range is determined by the considerable sparsity of contamination observed for this concentration rather than by the sensitivity of the AFM method. The sparsity necessitates increasing both the scanning area and the number of points where the measurement is taken from the surface, and this significantly complicates the measurement process.

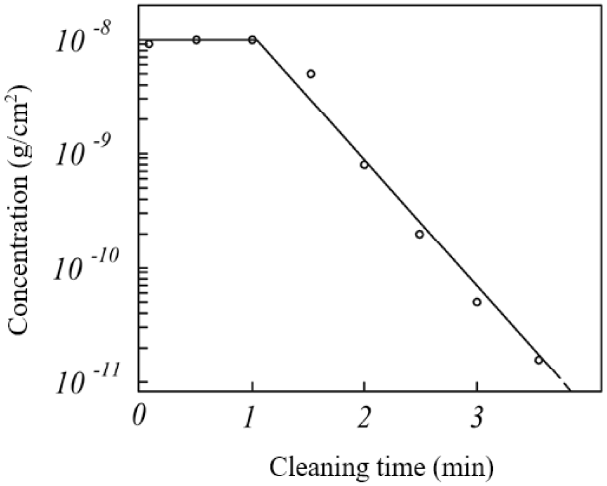

Figure 4. Relationship between the concentration of an organic contaminant and the time of irradiation in Solarus 950, obtained with the present method: the symbol ° denotes experimental values, and the continuous line shows the approximations of experimental data

For a cleaning time ranging from 0 to 1 min, the measured concentration remains constant and equals 10^{-8} g/cm^2. This means that the present method has a low sensitivity when the degree of contamination corresponds to the monomolecular film of the adsrobate. But surfaces with that amount of contamination are not of interest to modern micro- and nanostructuring technology.

CONCLUSION

In this paper, we looked into a method for determining the concentration of organic contaminants on the surfaces of semiconductor and dielectric materials, consisting of two stages. The first stage consists in making maps of lateral forces that act between the probe of the scanning probe microscope and the surface under study as well as in registering the typology of the same surface section. The second stage consists in analyzing both the maps and typology to determine the mass concentration of contaminants.

We have proved experimentally that the optimal frequency for scanning a surface is 1 Hz. Scanning at 1 Hz increases image contrast and facilitates interpreting data. The sensitivity of our method reaches 10^{-11} g/cm^2, a value that meets the modern requirements of micro- and nanostructuring technology.

ACKNOWLEDGMENT

The work was supported by RSF (project No. 18-12-00013).

REFERENCES

1. Rochat, N., Olivier, M., Chabli, A, Conne, F., Lefeuvre, G., & Boll-Burdet, C. (2000). Multiple internal reflection infrared spectroscopy using two-prism coupling geometry: A convenient way for quantitative study of organic contamination on silicon wafers. *Applied Physics Letters, 77*(14), 2249-2251. doi:10.1063/1.1314885
2. New ISO draft standard classifies surface particle cleanliness (2007). *Journal of IEST, 50*(2), 1–4. doi:10.17764/jiet.50.2.d622juj1548x2485
3. Zhang, X., & Chae, J. (2011). A wireless and passive wafer cleanliness monitoring unit via electromagnetic coupling for semiconductor/MEMS manufacturing facilities." *Sensors and Actuators A: Physical, 171*(2), 414–420. doi:10.1016/j.sna.2011.08.005
4. Soifer, V. A., ed. (2003). *Metody komp'yuternoy optiki [Methods of Computer Optics]*. Moscow: Fizmatlit (in Russian).
5. Kazanskiy, N. L., & Kolpakov, V. A. (2009). Microstructuring the surfaces of optical materials with a directed flux of off-electrode plasma: A Monograph. Moscow: Radio and Communications.
6. Goddard, J., Mandal, S., & Erickson, D. (2009). Optically resonant nanophotonic devices for label-free biomolecular detection. In *Advanced Photonic Structures for Biological and Chemical Detection*, 445–470. New York: Springer. doi:10.1007/978-0-387-98063-8
7. Lin, M. C., Wang, M. Q., Lai, J., Huang, R., Weng, C. M., Liao, J. H., Tang, J. S., Weng, C. H., Lu, W., Chen, H. W., & Lee, J. T. C. (2007). Metal hard mask employed Cu/Low *k* film post ash and wet clean process optimization and integration into 65 nm manufacturing flow. *Solid State Phenomena, 134*, 359–362. doi:10.4028/www.scientific.net/SSP.134.359
8. Liu, Y. J., Waugh, D. M., & Yu H. Z. (2002). Impact of organic contamination on the electrical properties of hydrogen-terminated silicon under ambient conditions. *Applied Physics Letters, 81*(26), 4967–4969. doi:10.1063/1.1532758
9. Alberici, S., Dellafiore, A., Manzo, G., Santospirito, G., Villa, C. M., & Zanotti, L. (2004). Organic contamination study for adhesion enhancement between final passivation surface and packaging molding compound. *Microelectronic Engineering, 76*(1–4), 227–234. doi:10.1016/j.mee.2004.07.040
10. Khanna, V. K. (2011). Adhesion–delamination phenomena at the surfaces and interfaces in microelectronics and MEMS structures and packaged devices. *Journal of Physics D: Applied Physics, 44*(3), 1–19. doi:10.1088/0022-3727/44/3/034004
11. Kim, K. S., Kim, J. Y., Kang, H. B., Lee, B. Y., & Park, S. M. (2008). Effects of organic contaminants during metal oxide semiconductor processes. *Journal of the Electrochemical Society, 155*(6), H426–H431. doi:10.1149/1.2904453
12. Guan, J. J., Gale, G. W., & Bennett, J. (2000). Effects of wet chemistry pre-gate clean strategies on the organic contamination of gate oxides for metal-oxide-semiconductor field effect transistor. *Japanese Journal of Applied Physics, 39*(7), 3947–3954. doi:10.1143/JJAP.39.3947
13. Tsai, C. L., Roman, P., Wu, C. T., Pantano, C., Berry, J., Kamieniecki, E., & Ruzyllo, J. (2003). Control of organic contamination of silicon surfaces using white light illumination in ambient air. *Journal of the Electrochemical Society, 150*(1), G39–G44.
14. Saga, K., & Hattori, T. (1996). Identification and removal of trace organic contamination on silicon wafers stored in plastic boxes. *Journal of the Electrochemical Society, 143*(10), 3279–3284. doi:10.1149/1.1837198
15. Reinhardt, K. A., & Kern, W. (2008). *Handbook of silicon wafer cleaning technology*. 2nd ed. Norwich, NY: William Andrew Publishing.
16. Chia, V. K. F. (2010) Process tool cleanliness for clean manufacturing. In *advanced Semiconductor manufacturing conference*, 79–83. IEEE. doi:10.1109/ASMC.2010.5551422

17. Endo, M., Yoshida, H., Maeda, Y., Miyamoto, N., & Niwano, M. (1999). Infrared monitoring system for the detection of organic contamination on a 300 mm Si wafer. *Applied Physics Letters, 75*(4). 519–521. doi:10.1063/1.124434

18. Liu, Y., Wu, T., & Evans, D. F. (1994). Lateral force microscopy study on the shear properties of self-assembled monolayers of dialkylammonium surfactant on mica. *Langmuir, 10*(7), 2241–2245. doi:10.1021/la00019a035

19. Dubravin, A. M., Komkov, O. Yu., & Myshkin, N. K. (2005). Local tribometry with the scanning probe microscope. *Trenie i iznos (Friction and Wear), 26*(3), 269–278.

20. Guo, Y. B., Wang, D. G., & Zhang, S. W. (2011). Adhesion and friction of nanoparticles/polyelectrolyte multilayer films by AFM and micro-tribometer. *Tribology International, 44*(7–8), 906–915. doi:10.1016/j.triboint.2011.03.007

21. Chernyaev, V. N. (1987). *Physical and chemical processes in electronics manufacture*. Moscow: Vysshaya shkola (in Russian).

22. Volkenstein, M. V. (1975). *Molecular biophysics*. Moscow: Nauka (in Russian).

23. Glinka, N. L. (2012). *General chemistry: a textbook*. Moscow: KnoRus (in Russian).

24. Podlipnov, V. V., & Dubovik, A. S. (2012). Matematicheskaya model' pribora kontrolya chistoty poverkhnosti podlozhek po skorosti rastekaniya kapli zhidkosti [A mathematical model for a device for assessing the cleanliness of substrate surfaces by the spread rate of a liquid drop]. *Nauchnoye priborostroyeniye [Scientiific Instrumental Engineering], 22*(2), 74-81 (in Russian).

25. Habuka, H., Naito, T., & Kawahara, N. (2010). Molecular interaction radii and rate constants for clarifying organic compound physisorption on silicon surface. *Journal of the Electrochemical Society, 157*(11), H1014–H1018. doi: 10.1149/1.3489364